

THE DISCOVERY AND MEASUREMENTS OF A HIGGS BOSON

F. GIANOTTI

PH Department, CERN, CH 121 Geneva 23, Switzerland

T. S. VIRDEE

Imperial College, London SW7 2BZ, U.K.,

In July 2012, the ATLAS and CMS collaborations at CERN's Large Hadron Collider announced the remarkable discovery of a Higgs-like boson, a new heavy particle at a mass more than 130 times the mass of a proton. Since then, further data have revealed its properties to be strikingly similar to those of the Standard Model Higgs boson, a particle expected from the mechanism introduced almost 50 years ago by six theoreticians including British physicists Peter Higgs from Edinburgh University and Tom Kibble from Imperial College. The discovery is the culmination of a truly remarkable scientific journey and undoubtedly the most significant scientific discovery of the 21st century so far. Its experimental confirmation turned out to be a monumental task requiring the creation of an accelerator and experiments of unprecedented capability and complexity, designed to discern the signatures that correspond to the Higgs boson. Thousands of scientists and engineers, in each of the ATLAS and CMS teams, came together from all four corners of the world to make this massive discovery possible.

Keywords: LHC; ATLAS; CMS; Standard Model; Higgs boson.

1. Introduction

The Standard Model (SM) of particle physics has emerged through both theoretical and experimental discoveries spanning the last five decades. It comprises the building blocks of visible matter, the fundamental fermions, quarks and leptons, and the fundamental bosons that mediate three of the four fundamental interactions; photons for electromagnetism, the W and Z bosons for the weak interaction and gluons for the strong interaction [1]. The photon is massless whilst the W and Z bosons acquire mass through a spontaneous symmetry-breaking mechanism proposed by three groups of physicists (Englert and Brout; Higgs; and Guralnik, Hagen, and Kibble) [2-7]. This is achieved through the introduction of a complex scalar field leading to an additional massive scalar boson, labeled the SM Higgs boson. The fundamental fermions acquire mass through a Yukawa interaction of the Higgs boson. Only the gravitational interaction remains outside the SM.

The year 2013 marked the 30th anniversary of the discovery of the W and Z bosons by the UA1 and UA2 experiments at the proton-antiproton collider at CERN. The discovery of the W and Z bosons focused efforts, and set the stage, for the search for the Higgs boson. In the following year, 1984, a workshop was held in Lausanne where first ideas were discussed about a possible high-energy proton-proton collider and associated experiments for this search. Amongst the leading protagonists were the scientists from the UA1 and UA2 experiments. The aim was to reuse the LEP tunnel after the end of the electron-positron programme. An exploratory machine was required to cover the wide range of mass, the diverse signatures and mechanisms thought to be effective for the production of new particles at a centre-of-mass energy ten times higher than previously had been probed. A hadron (proton-proton) collider is such a machine as long as the proton energy is high enough and the instantaneous proton-proton interaction rate is sufficiently large. The centre of mass energy was set at 14 TeV and the rate at 1 billion pairs of protons interacting every second (corresponding to a luminosity $\mathcal{L} = 10^{34} \text{ cm}^{-2}\text{s}^{-1}$). The hadron colliders can provide these conditions though at the expense of ‘clean’ experimental conditions due to multiple interactions in every bunch crossing.

Some of the physics questions the particle physics community was pondering over are listed below.

A key aim was to clarify symmetry breaking in the electro-weak sector, most likely requiring a search for the SM Higgs boson.

At very high energies, such as at the Large Hadron Collider (LHC), the probability of some fundamental processes such W_L - W_L scattering violates unitarity i.e. the probability becomes greater than one - that obviously would not make sense. A process involving the exchange of a Higgs boson would be able to “regulate” the process and give a finite answer.

Furthermore it was known that the discovery of a fundamental scalar (spin 0) Higgs boson would raise another deep question – why would the mass of such a Higgs boson lie in the range probed by the LHC. Quantum corrections make the mass of a fundamental scalar particle float up to the next highest physical mass scale that, in the absence of extensions to the SM, could be as high as 10^{16} GeV. It is widely believed that the answer to this question would lie in new physics beyond the SM (BSM). One appealing hypothesis, much discussed at the time, and still being investigated, predicts a new symmetry labeled *supersymmetry*. For every known SM particle there would be a partner with spin differing by half a unit; fermions

would have boson partners and vice versa, thus doubling the number of fundamental particles. The contributions from the boson and fermion superpartners, and vice a versa, would lead to cancellations and allow the existence of a low mass for the Higgs boson. In the simplest forms of supersymmetry five Higgs bosons are predicted to exist with one resembling the SM Higgs boson with a mass below ~ 140 GeV. The lightest of this new species of super-particles could be the candidate for *dark matter* in the universe that is around five times more abundant than ordinary matter.

Also it was clear that a search had to be made for new physics at the TeV energy scale as the SM is logically incomplete; it does not incorporate gravity. Superstring theory is an attempt towards a unified theory with dramatic predictions of extra space dimensions and supersymmetry.

The LHC and its experiments [8] were designed to find new particles, new forces and new symmetries, amongst which could be the Higgs boson(s), supersymmetric particles, Z' bosons, or evidence of extra space dimensions. An experiment that could cover the detection of all these “known” but yet undiscovered particles, or phenomena, would also allow discovery of whatever else Nature has in store at the LHC energies.

2. The Standard Model Higgs boson and the LHC.

The mass of the Higgs boson is not predicted by theory but for a given mass all of its other properties are precisely predicted. From general considerations $m_H < 1$ TeV whilst precision electroweak constraints imply that $m_H < 152$ GeV at 95% confidence level (CL) [9, 10]. The lower limit on the mass of the Higgs boson from the LEP experiments was 114.4 GeV [10, 11].

Once produced the Higgs boson disintegrates immediately in one of several ways (decay modes) into known SM particles, depending on its mass. A search had to be envisaged not only over a large range of masses but also many possible decay modes: into pairs of photons, Z bosons, W bosons, τ leptons, and b quarks.

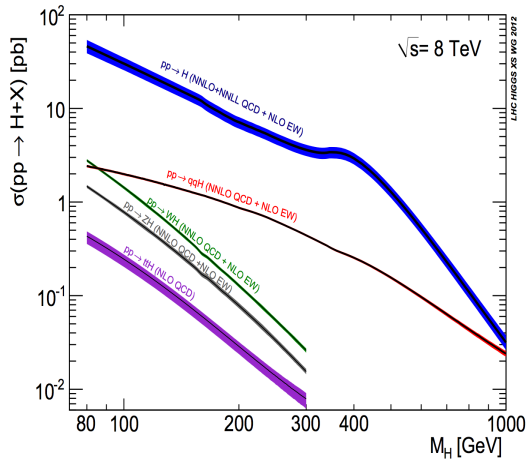


Figure 1a: The SM Higgs boson production cross-section at $\sqrt{s} = 8$ TeV as a function of mass.

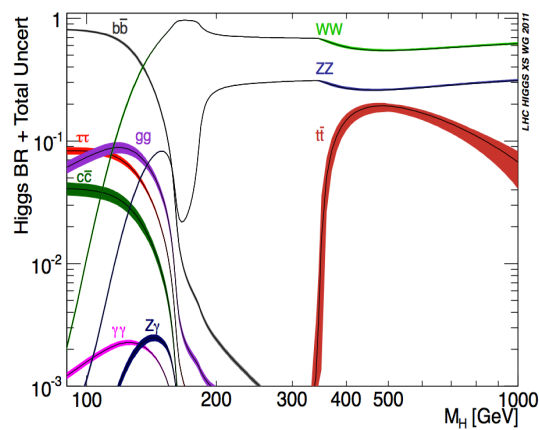


Figure 1b: The SM Higgs boson branching ratios as a function of mass.

The production cross sections and the branching ratios into the various decay modes of the SM Higgs boson as a function of mass are illustrated in Figs. 1a, b, respectively [12]. The dominant Higgs boson production mechanism, for masses up to ≈ 700 GeV, is gluon–gluon

fusion. The W–W or Z–Z fusion mechanism, known as vector boson fusion (VBF), becomes important for the production of higher-mass Higgs bosons. Here, the quarks that emit the W/Z bosons end up in the final states with transverse momenta of the order of W and Z masses. The detection of the resulting high-energy jets in the forward regions, $2.0 < |\eta| < 5.0^1$, can be used to tag the reaction, improving the signal-to-noise ratio and extending the mass range over which the Higgs boson can be discovered. These tagging jets turned out also to be very important in the measurements of the properties of the newly found boson. ~~These jets are highly boosted and their transverse size is similar to that of a high energy hadron shower.~~

3. Timeline of the Large Hadron Collider project

In the late 1980's and early 1990's [13-15] several workshops and conferences took place where the formidable experimental challenges [16] at a high energy, high luminosity, hadron collider started to appear manageable, provided that enough R&D work could be carried out, especially on detectors.

The search for the SM Higgs boson played a vital role in the design of the general-purpose detectors. A search had to be made across the entire allowed range of masses; from around a mass of ~ 50 GeV, the lower limit at the time, up to its largest possible value of around 1000 GeV.

In 1990, at a seminal meeting in Aachen, discussions focused on the physics potential, the detector technologies and magnetic field configurations in possible experiments. The natural width of the SM Higgs boson in the low mass region is very small (< 10 MeV $\Rightarrow \Gamma_H/m_H \sim 10^{-4}$). Hence the width of any observed peak would be entirely dominated by instrumental mass resolution. Considerable emphasis was therefore put on the value of the magnetic field strength, on the precision charged particle tracking systems and on high-resolution calorimeters.

In 1992 four experiment designs were presented at a meeting in Evian: two deploying toroids (one superconducting) and two deploying superconducting high-field solenoids. In June 1993 CERN's scientific peer review committee, the LHC Committee (LHCC), recommended that the ATLAS and CMS experiments proceed further to the next phase of technical proposals.

In the 1990's the two collaborations grew most rapidly in terms of people and institutes. Finding new collaborators was high on the "to do" list of the leaders of the experiments.

The formal approval for construction was given in July 1997 by the then director-general, Chris Llewellyn Smith, imposing a material cost ceiling of 475 MCHF.

The magnitude of the challenge is captured by a saying prevalent in the late 1980's and early 1990's - 'We think we know how to build a high energy, high luminosity hadron collider – but we don't have the technology to build a detector for it'. Many technical, financial, industrial and human challenges lay ahead which were all overcome to yield experiments of unprecedented complexity and power. A flavour can be attained from articles in reference [17].

After the formal approval an intense ten-year period of construction ensued. In 2008 the LHC experiments were ready for pp collisions.

¹ The pseudorapidity, η , is defined as $\eta = -\ln[\tan(\theta/2)]$ where θ is the polar angle measured from the positive z axis (along the anticlockwise beam direction).

Mention also LHCb and ALICE at least once ?

3.1 The ATLAS and CMS experiments [18]

Arguably the most important aspect of experiment design and layout at hadron colliders is the choice of the configuration of the magnetic field for the measurement of the momentum of muons. Large bending power is needed to measure, with sufficient precision, the momentum of charged particles. This forces a choice of superconducting technology for the magnets.

The ATLAS design (Fig. 2) [19] centred on three very large superconducting air-core toroids for the measurement of muons, supplemented by a superconducting 2 Tesla solenoid to provide the magnetic field for inner tracking and by a liquid-argon/lead electromagnetic calorimeter with a novel “accordion” geometry. The CMS design (Fig. 3) [20], in a complementary design, was based on a single large-bore, long, high-field solenoid for analyzing muons, together with powerful silicon microstrip-based inner tracking and an electromagnetic calorimeter of scintillating crystals.

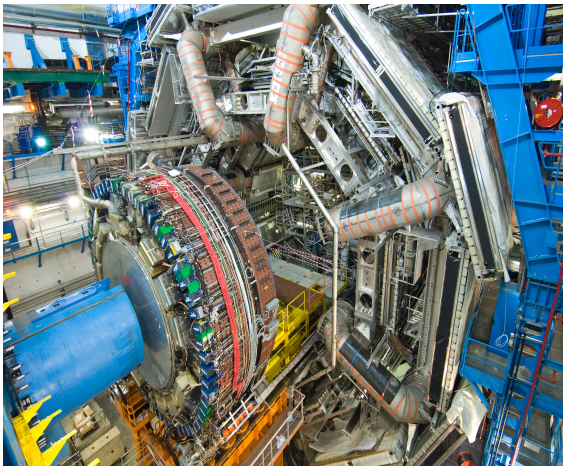


Figure 2: A view of the ATLAS experiment during construction.

Figure 3: A transverse view of the CMS experiment during construction.

The CMS and ATLAS detectors have performed very well, and according to the ambitious design specifications laid down in the mid-1990’s. They are the most sophisticated general-purpose particle physics experiments ever built. They were rapidly commissioned and started producing publishable physics results within a few months of recording first pp collisions

In order to discover the new phenomena mentioned above protons have to collide head on; in fact the partons inside the protons (quarks and gluons) have to collide head-on, in what is termed a “hard interaction” (Fig. 4), as opposed to a glancing collision where less energy is involved in the physics of the interaction. Any new particles produced as a result of these collisions will manifest themselves through disintegration into the well known particles of the SM mentioned above. The photons, electrons and muons can emerge into the detectors directly from the hard interaction, whereas quarks and gluons, never visible as free particles, appear in the detectors as collimated bunches of stable or quasi-stable particles labeled “jets”.



Figure 4: An event display of a “hard” proton-proton collision in CMS illustrating the inner tracking detector hits (yellow) and the energy deposits in the electromagnetic calorimeter (red) and the hadron calorimeter (blue). The height of the red and blue towers is indicative of the energy deposited. The muon system is not displayed. The production of “jets” is evident from the collimated bunches of particles.

Figure 5 shows the distribution of effective masses of all di-muon pairs detected in CMS upon examination of the first 3 trillion proton-proton interactions. The sharpness of the peaks, corresponding to the labeled particle states, depends on the natural width of the state under study, defined as $\Gamma = \hbar/2\pi\tau$, where τ is the lifetime of the particle, and/or on the experimentally achievable mass resolution.

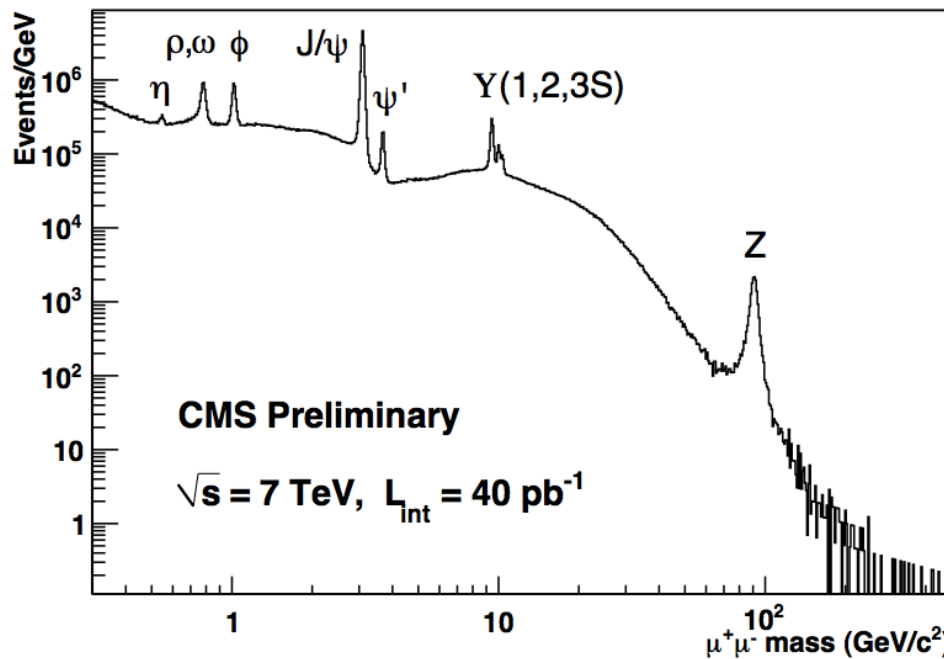


Figure 5: The distribution of di-muon effective masses showing the various resonant states. The mass

resolutions in the central region are: 28 MeV (0.9%) for J/ψ , 69 MeV (0.7%) for $Y(1S)$, both dominated by instrumental resolution, and $\Gamma=2.5$ GeV for the Z dominated by its natural width.

For example, as can be seen in Fig. 5, the observed width of particles such as J/ψ or Y is dominated by the instrumental resolution whilst that of the Z by its natural width. The background can also be seen and the clarity (high signal over background) of the signals is evident. It is remarkable that the ATLAS and CMS experiments, arguably the most technologically challenging scientific instruments ever built, achieved their design mass resolutions after the first few months of data-taking.

4. First data and first physics results

After a short low-energy run in 2009, the LHC physics journey started in earnest in April 2010, when first proton-proton collisions at an unprecedented centre-of-mass energy ($\sqrt{s} = 7$ TeV, 3.5 times larger than at the previous most powerful hadron collider, the Tevatron at Fermilab) inaugurated the exploration of a new energy scale. The collision energy was raised to $\sqrt{s} = 8$ TeV in 2012. The first LHC data-taking period (so-called “Run 1”) covered about four years, from April 2010 to February 2013.

Large amounts of data, about 5 billion events, were recorded by each of ATLAS and CMS in Run 1. They include, for each experiment and after the main selections of the analysis, about 100 million $W \rightarrow l\nu^2$ events, 10 million $Z \rightarrow ll$ decays, half a million top-quark pair events with at least one lepton in the final state, etc. Such datasets exceed, in some cases by orders of magnitude, the size of the samples recorded by the CDF and D0 experiment at the Tevatron during the whole lifetime of that project. They have enabled detailed measurements of a large variety of SM processes in a new energy regime, searches for physics beyond the SM, with null results so far [21-22], and the discovery of a new particle compatible with the SM Higgs boson. By the time of the Royal Society meeting (January 2013), ATLAS and CMS had each submitted about 270 articles for publication on peer-reviewed journals.

These extraordinary accomplishments on a short time scale are the result of the competence and dedication of the scientists involved in the ATLAS and CMS experiments, and of the excellent performance, right from the beginning, of the LHC accelerator, detectors, and computing infrastructure. These key “ingredients” are discussed briefly below.

ATLAS and CMS consist of about 3000 scientists each, from about 40 countries. Figure 6 shows the age distribution of the ATLAS Collaboration: about half of the physicists are below age 35, and about 30% are PhD students. The fraction of women is 20% on average, larger in the young generations.

In 2012, the LHC [23] achieved the record instantaneous luminosity of $\mathcal{L} = 7 \times 10^{33} \text{ cm}^{-2} \text{ s}^{-1}$ by circulating high-intensity beams consisting of about 1300 bunches separated by 50 ns, with 150 billion protons per bunch, and a transverse size of about 20 μm when colliding in ATLAS and CMS. The luminosity integrated over time delivered to each experiment during Run 1 was about $\int \mathcal{L} dt \sim 30 \text{ fb}^{-1}$, most of which at $\sqrt{s} = 8$ TeV. Since the number of events (N) produced by a specific physics process with cross section σ is given by $N = \sigma \int \mathcal{L} dt$, physics reach, in particular the possibility of observing rare processes with small cross sections such as a heavy (new) particle, demands large integrated luminosities, i.e. high instantaneous luminosities and minimization of the accelerator downtime. Although essential

² Unless otherwise stated, the lepton symbol l indicates an electron or a muon

for physics, the high luminosities achieved in Run 1 gave rise to a harsh experimental

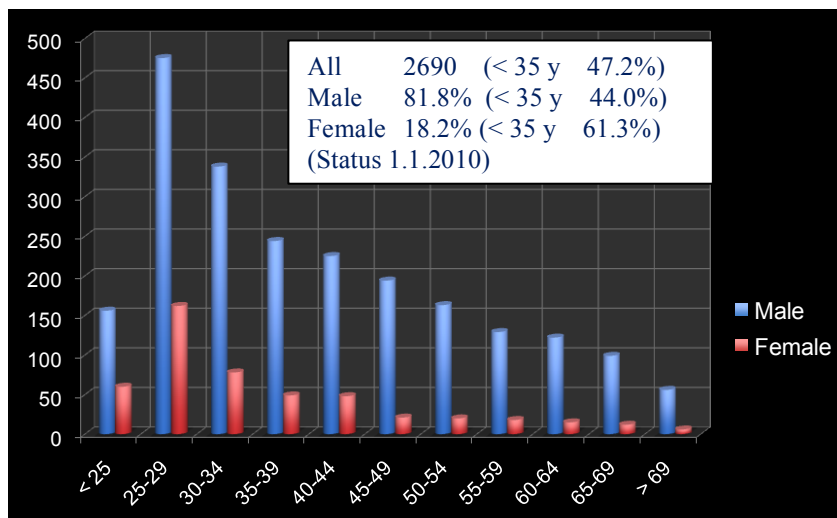


Figure 6: The age distribution of the ATLAS Collaboration physicists for males (blue) and females (red).

environment, and ATLAS and CMS had to deal with a large number of simultaneous proton-proton interactions (so-called “pile-up”) produced, at each beam crossing every 50 ns, by the very dense colliding bunches. The challenge is illustrated in Fig. 7.



Figure 7: Displays of events recorded by ATLAS in 2010 (left panel), 2011 (middle panel) and 2012 (right panel). Trajectories of charged particles with $p_T > 0.4$ GeV are shown in transverse views of the tracking detectors. The yellow tracks in the right panel indicate the two muons produced from a $Z \rightarrow \mu\mu$ decay.

In 2010 the instantaneous luminosity was about $\mathcal{L} \sim 10^{32} \text{ cm}^{-2} \text{ s}^{-1}$, and typically two interactions were produced at each bunch crossing: the resulting events were pretty clean, as shown in the left panel in Fig. 7. In 2011, the event complexity increased, due to the number of overlapping interactions reaching about ten per crossing (middle panel). Finally in 2012, with luminosities above $5 \times 10^{33} \text{ cm}^{-2} \text{ s}^{-1}$ and an average of 20 pile-up collisions per crossing, extraction and measurements of the interesting hard interactions required the full power of the detectors and a lot of inventiveness at the analysis level.

Concerning the detectors, examples of their excellent operational performance include: a data-taking efficiency (this is the fraction of delivered luminosity recorded by the experiments) well above 90%; a fraction of non-operational channels between a few permil

and a few percent (Fig. 8); and a data quality (the fraction of recorded data good enough to be used for physics studies) of about 95%. High efficiencies are crucial because some of the interesting processes, for instance Higgs boson production followed by decay into four leptons ($H \rightarrow 4l$), are extremely rare: only a handful of $H \rightarrow 4l$ events had been recorded by each experiment at the time of the announcement of a Higgs-like boson in July 2012. Such a remarkable operation performance for experiments of the complexity of ATLAS and CMS testifies to the excellent quality of the construction and the powerful control and calibration systems.

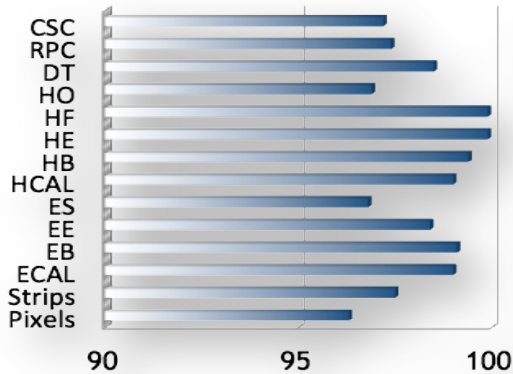


Figure 8: Fraction of operating channels for the various detector components of the CMS experiment.

The LHC computing infrastructure is based on a network of 135 sites distributed in 35 countries across the globe, the so-called worldwide LHC Computing Grid (wLCG). The wLCG provides resources for data storage and analysis, integrated into a single system accessible in a seamless way by all scientists involved in the LHC. The challenges are daunting also in this case, as about 200 PB of disk space are required to store the huge amount of LHC data, and 350000 CPU cores to process and analyze them. In 2012, the LHC was ranked among the top-ten producers of big data in the world. Since the beginning of the LHC operation, the wLCG has allowed users from all over the world to access the data shortly after they were recorded and to do analysis in an effective manner. Today the grid is used also in other fields, from archeology to finance and life sciences.

5. Standard Model measurements

Thanks to the excellent performance described in the previous Section, ATLAS and CMS were able to “reproduce” fifty years of particle physics in less than one year of operation, as illustrated in Fig. 9. The W and Z bosons and the top quark were detected already in the first half of 2010, and since then have been measured with increasing precision. For instance, the top-quark mass is known today with an uncertainty of a few permil from the Tevatron and the LHC, as shown in Fig. 10. The top quark is the heaviest elementary particle ever observed, with a mass comparable to that of a gold atom. It decays before hadronising, and plays a special role in radiative corrections [24]. It is therefore a very intriguing particle, which could offer a doorway to physics beyond the Standard Model, and needs to be measured with the highest precision. The results reported in Fig. 10 are a further demonstration of the excellence of the LHC detectors and software tools (simulation, reconstruction, etc.). Indeed, events due to the production and decay of top-quark pairs contain all main physics objects (leptons, jets,

b-quark jets, missing transverse energy), all of which must be measured

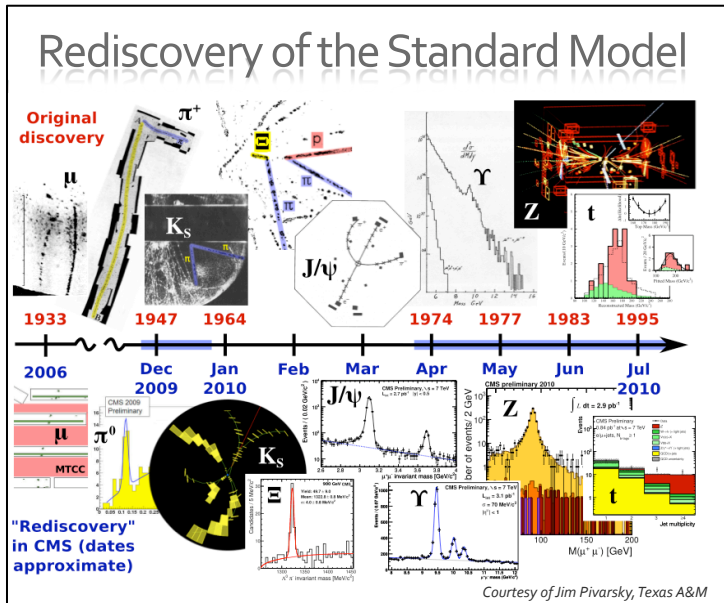


Figure 9: Top: main milestones of the experimental history of the Standard Model through the discovery signals of several important particles as a function of time. Bottom: signals of the same particles as detected in the CMS experiment with early data.

extremely well, and with an excellent control of the related systematic uncertainties, to be able to achieve such an exquisite precision on the determination of the top-quark mass.

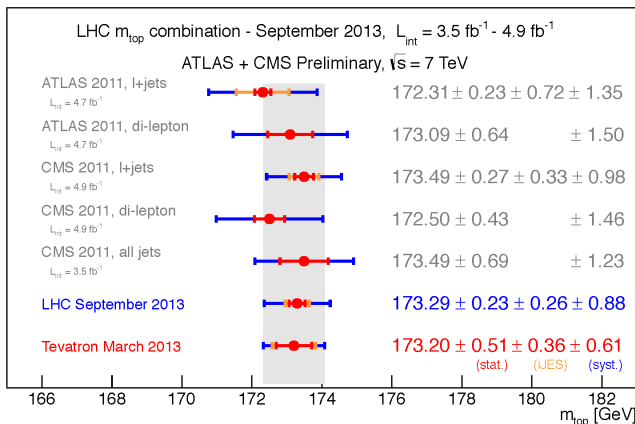


Figure 10: Measurements of the top-quark mass by ATLAS and CMS in various final states and their combination. The combined measurement of the CDF and D0 experiments at the Tevatron is also shown [25].

ATLAS and CMS have also measured the production cross sections for the main SM processes, both for inclusive final states as well as topologies where the main particle is accompanied by jets (Fig. 11). As another example, Fig. 12 shows the production of jets over an energy range from 80 GeV to 2 TeV and in different angular regions of the detector. The SM predictions are in excellent agreement with the data, in some cases over cross section ranges of several orders of magnitude. These results are also very useful to improve the theoretical description of the physics (including parton distribution functions, underlying

event, initial- and final-state jet radiation) in the Monte Carlo generators used to simulate the various processes.

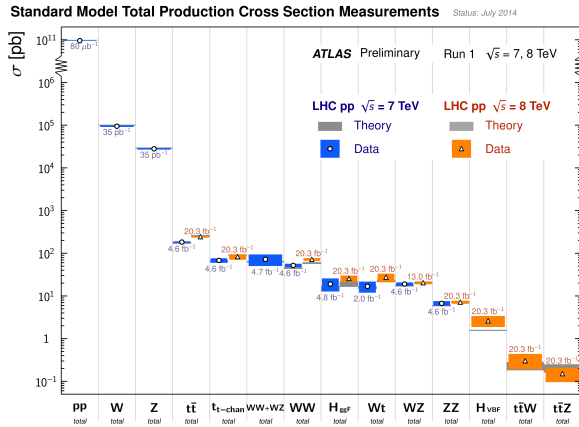


Figure 11: Measurements of the total production cross sections for several SM processes in ATLAS, compared to the corresponding next-to-leading order theoretical expectations. The integrated luminosity used for each measurement is indicated close to the data point.

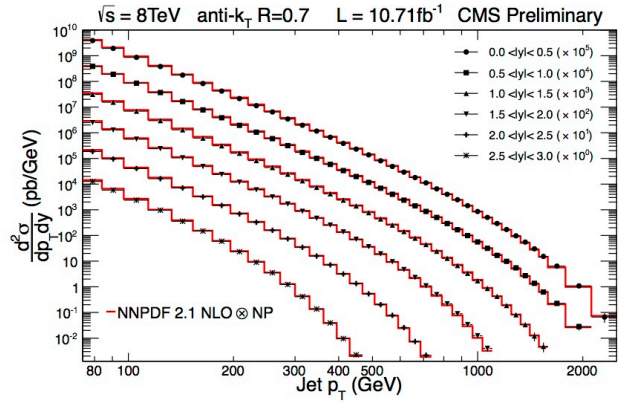


Figure 12: Jet production cross section measured in CMS in various rapidity regions (indicated by the various symbols), compared to the next-to-leading order SM theoretical expectation (full lines) [26].

In conclusion, the Standard Model works beautifully also in the (new) energy range explored by the LHC. Indeed, no significant deviations from its predictions have been observed so far. Furthermore, because most of the known processes are important backgrounds to searches for new particles, including the Higgs boson, SM measurements are an essential prerequisite for the experiments to be able to observe an undisputable signal. Armed with these solid foundations, ATLAS and CMS were ready to undertake the path toward the Higgs boson discovery.

6. The Discovery of a Higgs boson

Undoubtedly, the most striking result to emerge from the ATLAS [27] and CMS [28] experiments is the discovery of a new heavy boson with a mass of ~ 125 GeV. The analysis was carried out in the context of the search for the SM Higgs boson.

The predicted rate of production of the SM Higgs bosons, its decay modes and its natural width vary widely over the allowed mass range (100–1000 GeV). It couples to the different pairs of particles in a proportion that is precisely predicted by the SM, i.e. for fermions (f) proportional to m_f^2 and for bosons (V) proportional to m_V^4/v^2 where v is the vacuum expectation value of the scalar field ($v=246$ GeV). For example, at $m_H=125$ GeV the SM boson is predicted to decay into pairs of photons with a branching ratio, $BR=2.3 \times 10^{-3}$, into Z bosons and then four electrons or muons or two muons and two electrons with $BR=1.25 \times 10^{-4}$, into a pair of W bosons and then into $ll\nu\nu$ with $BR \sim 1\%$, a pair of τ -leptons with $BR=6.4\%$, and into a pair of b-quarks with $BR=54\%$.

For a given Higgs boson mass hypothesis, the sensitivity of the search depends on:

- the mass of the Higgs boson,
- the Higgs boson production cross section (Fig. 1a),
- the decay branching fraction into the selected final state (Fig. 1b),
- the signal selection efficiency,
- the expected Higgs boson experimental mass resolution and
- the level of backgrounds with the same or a similar final state

To improve sensitivity events are separated into categories with different S/B and analysed independently. For many analyses all relevant information on signal v/s background discrimination (aside from mass itself) is encoded into a multivariate (MVA) output independent of mass.

In 2011 the ATLAS and CMS experiments recorded data corresponding to an integrated luminosity of $\sim 5 \text{ fb}^{-1}$ at $\sqrt{s}=7 \text{ TeV}$. In December 2011, first “tantalizing hints” of a new particle from both the CMS and ATLAS experiments were shown at CERN. The general conclusion was that both experiments were seeing an excess of unusual events at roughly the same place in mass (in the mass range 120-130 GeV) in two different decay channels. That set the stage for data taking in 2012.

In January 2012 it was decided to slightly increase the energy of the protons from 3.5 to 4 TeV, giving a centre of mass energy of 8 TeV. By June 2012 the number of high-energy collisions examined had doubled and both CMS and ATLAS had greatly improved their analyses. It was decided to look at the region that had shown the excess of events but only after all the algorithms and selection procedures had been agreed, in case a bias was inadvertently introduced. These data led to the discovery of a Higgs boson, independently in both the ATLAS and CMS experiments in July 2012 (see Section 6.1).

In what follows we shall concentrate on the region of low mass ($114 < m_H < 150 \text{ GeV}$) where the two channels particularly suited for unambiguous discovery are the decays to two photons and to two Z bosons, where one or both of the Z bosons could be virtual, subsequently decaying into four electrons, four muons or two electrons and two muons. These are particularly suited as the observed mass resolution ($\sim 1\%$ of m_H) is the best and the backgrounds manageable or small.

By the end of 2012 (LHC Run 1) the total amount of data that had been examined corresponded to $\sim 5 \text{ fb}^{-1}$ at $\sqrt{s}=7 \text{ TeV}$ and $\sim 20 \text{ fb}^{-1}$ at $\sqrt{s}=8 \text{ TeV}$, equating to the examination of some 2000 trillion proton-proton collisions, potentially producing 600k SM Higgs bosons in each of the two experiments. Using these data first measurements of the properties of the new boson were also made (see Section 6.2).

All kinematic distributions shown below have been produced after all the selection cuts have been applied.

6.1 The discovery of a Higgs boson: results from 2011 and partial 2012 datasets

In this section we discuss the analyses that led to the discovery of a new heavy boson around a mass of 125 GeV, using the data accumulated up to June 2012.

6.1.1 The $H \rightarrow \gamma\gamma$ decay mode

In the $H \rightarrow \gamma\gamma$ analysis a search is made for a narrow peak in the diphoton invariant mass distribution in the mass range 110–150 GeV, on a large predominantly irreducible

background from QCD production of two photons (via quark-antiquark annihilation and “box” diagrams). There is also a reducible background where one or more of the reconstructed photon candidates originate from misidentification of jet fragments, with the process of QCD Compton scattering dominating.

A candidate event recorded in the CMS detector is shown in Figure 13.

The event selection requires two photon candidates satisfying p_T and photon identification criteria. In CMS [28] a p_T threshold of $m_{\gamma\gamma}/3$ ($m_{\gamma\gamma}/4$) is applied to the photon leading (sub-leading) in p_T , where $m_{\gamma\gamma}$ is the diphoton invariant mass. Scaling the p_T thresholds in this way avoids distortion of the shape of the $m_{\gamma\gamma}$ distribution. The background is estimated from data, without the use of MC simulation, by fitting the diphoton invariant mass distribution in a range ($100 < m_{\gamma\gamma} < 180$ GeV). A polynomial function is used to describe the shape of the background.

The results from the CMS experiments are shown in Fig. 15. A clear peak at a diphoton invariant mass of around 125 GeV is seen. A similar result was obtained in the ATLAS experiment [27].

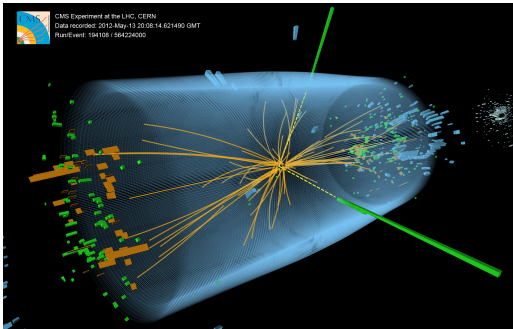


Figure 14: Event recorded with the CMS detector in 2012 at a proton-proton centre-of-mass energy of 8 TeV. The event shows characteristics expected from the decay of the SM Higgs boson to a pair of photons (dashed yellow lines and green towers). Solid yellow lines represent the reconstructed trajectories of the charged particles produced in addition to the two photons in the same collision. The event could also be due to known SM background processes.

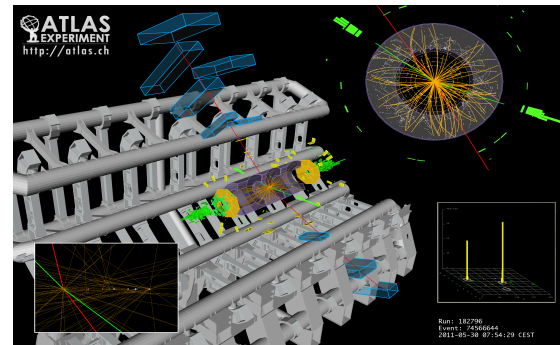


Figure 16: Event recorded with the ATLAS detector in 2012 at a proton-proton centre-of-mass energy of 8 TeV. The event shows characteristics expected from the decay of the SM Higgs boson to a pair of Z bosons, which in turn decay to a pair of electrons (green tracks and towers) and a pair of muons (red tracks). The event could also be due to known SM background processes.

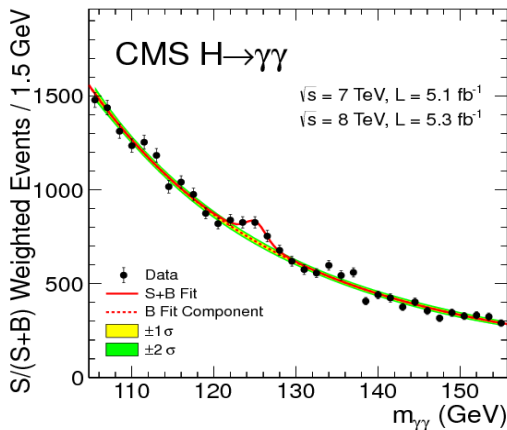


Figure 15: The two-photon invariant mass distribution of selected candidates in the CMS experiment, weighted by S/B of the category in which it falls. The lines represent the fitted background and the expected signal contribution ($m_H=125$ GeV).

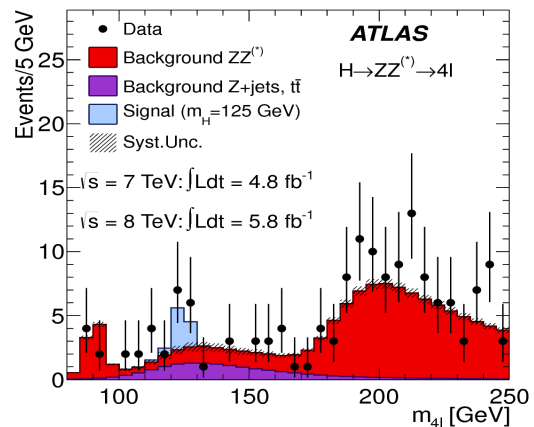


Figure 17: The four-lepton invariant mass distribution in the ATLAS experiment for selected candidates relative to the background expectation. The expected signal contribution ($m_H=125$ GeV) is also shown.

6.1.2 The $H \rightarrow ZZ \rightarrow 4l$ decay mode

In the $H \rightarrow ZZ \rightarrow 4l$ decay mode a search is made for a narrow four-charged lepton mass peak in the presence of a small continuum background. The background sources include an irreducible four-lepton contribution from direct ZZ production via quark-antiquark and gluon-gluon processes. Reducible background contributions arise from $Z + b\bar{b}$ and $t\bar{t}$ production where the final states contain two isolated leptons and two b-quark jets producing secondary leptons.

The event selection requires two pairs of same-flavour, oppositely charged leptons. Since there are differences in the reducible background rates and mass resolutions between the sub-channels $4e$, 4μ , and $2e2\mu$, they are analysed separately. Electrons are typically required to have $p_T > 7$ GeV. The corresponding requirements for muons are $p_T > 5-6$ GeV. Both electrons and muons are required to be isolated. The pair with invariant mass closest to the Z boson mass is required to have a mass in the range 40–120 GeV and the other pair is required to have a mass in the range 12–120 GeV. The ZZ background, which is dominant, is evaluated from Monte Carlo simulation studies.

Refer to fig. 16 (otherwise never called) ?

The m_{4l} distribution from the ATLAS experiment is shown in Fig. 17 [27]. A clear peak is observed at ~ 125 GeV in addition to the one at the Z mass. The latter is due to the conversion of an inner bremsstrahlung photon emitted simultaneously with the dilepton pair. A similar result was obtained by the CMS experiment [28].

6.1.3 Combinations

A search was also made in other decay modes of a possible Higgs boson and combined to yield the final results published in August 2012 by ATLAS [27] and CMS [28]. The observed (expected) local significances were 6.0σ (5.0σ) and 5.0σ (5.8σ) in ATLAS and CMS respectively. It was clear that both ATLAS and CMS independently discovered a new heavy boson at approximately the same mass, clearly evident in the same two different decay

modes, $\gamma\gamma$ and ZZ .

The decay into two bosons (two γ ; two Z bosons; two W bosons) implied that the new particle is a boson with spin different from one and its decay into two photons that it carries either spin-0 or spin-2.

The results presented by both ATLAS and CMS Collaborations were consistent, within uncertainties, with the expectations for a SM Higgs boson. Both noted that collection of more data would enable a more rigorous test of this conclusion and an investigation of whether the properties of the new particle imply physics beyond the SM.

6.2 Results from the full 2011 and 2012 data set - Properties

We present here the results from the full dataset corresponding to an integrated luminosity of $\sim 5 \text{ fb}^{-1}$ at $\sqrt{s}=7 \text{ TeV}$ and $\sim 20 \text{ fb}^{-1}$ at $\sqrt{s}=8 \text{ TeV}$. This larger dataset allowed confirmation of the discovery of the new boson, a better examination of the decay channels other than the $H \rightarrow \gamma\gamma$ and the $H \rightarrow ZZ \rightarrow 4l$ decay modes and the first substantial investigations of the boson's properties.

6.2.1 The $H \rightarrow \gamma\gamma$ and the $H \rightarrow ZZ \rightarrow 4l$ decay modes

The results from the ATLAS experiment are shown for the $H \rightarrow \gamma\gamma$ decay mode (Fig. 18) [29] and those from the CMS experiment for the $H \rightarrow ZZ \rightarrow 4l$ mode (Fig. 19) [30]. The signal is unmistakable and the significances have increased (see Section 7). The data show an even clearer excess of events above the expected background around 125 GeV. The complementary results from the two experiments can be found in references [31] and [29].

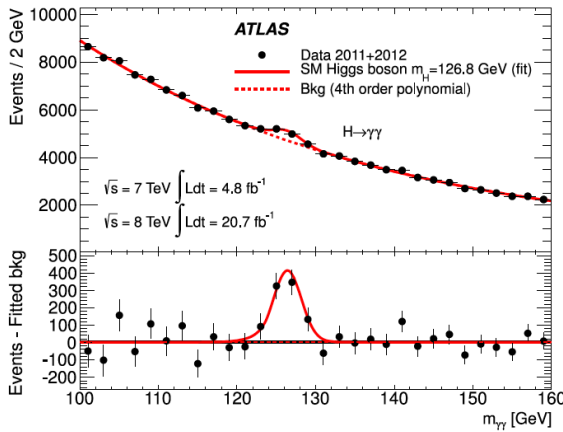


Figure 18: Invariant mass distribution of diphoton candidates. The result of a fit to the background described by a polynomial and the sum of signal and background components is superimposed. The bottom inset displays the residuals of the data with respect to the fitted background component.

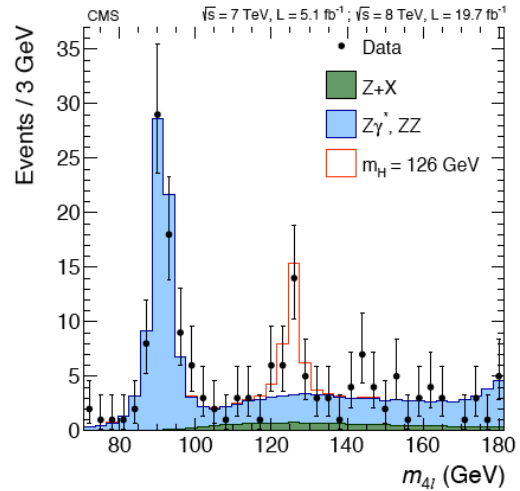


Figure 19: The four-lepton invariant mass distribution in the CMS experiment for selected candidates relative to the background expectation. The expected signal contribution is also shown.

6.2.2 $H \rightarrow WW \rightarrow 2l 2\nu$ decay mode

The search for $H \rightarrow W^+W^-$ is based on the study of the final state in which both W bosons decay leptonically, resulting in a signature with two isolated, oppositely charged, high p_T leptons (electrons or muons) and large missing transverse momentum, E_T^{miss} , due to the undetected neutrinos. The signal sensitivity is improved by separating events according to lepton flavor into e^+e^- , $\mu^+\mu^-$, and $e\mu$ samples and according to jet multiplicity into 0-jet and 1-jet samples. The dominant background arises from irreducible non-resonant WW production.

The m_{ll} distribution in the 0-jet and different-flavor final state is shown for CMS in Fig. 20 [32]. The expected contribution from a SM Higgs boson with $m_H = 125$ GeV is also shown. The transverse mass, m_T , distribution and the background-subtracted m_T distribution are shown in Fig. 21 for the ATLAS experiment [29]. The hatched areas represent the total uncertainty on the sum of the signal and background yields from statistical, experimental, and theoretical sources. Both show a clear excess of events compatible with a Higgs boson with mass ~ 125 GeV. The observed (expected) significance of the excess with respect to the background only hypothesis at a mass of 125.5 is 3.8 (3.8) standard deviation in the ATLAS experiment [29] and **3.9 (5.3)** standard deviations in the CMS experiment [32].

6.2.3 The $H \rightarrow \tau\tau$ decay mode

The $H \rightarrow \tau\tau$ search is performed using the final-state signatures ee , $e\mu$, $\mu\mu$, $e\tau_h$, $\mu\tau_h$, $\tau_h\tau_h$, where electrons and muons arise from leptonic τ -decays and τ_h denotes a τ lepton decaying hadronically. Each of these categories is further divided into two exclusive sub-categories based on the number and the type of the jets in the event: (i) events with one forward and one backward jet, consistent with the VBF topology, (ii) events with at least one high p_T hadronic jet but not selected in the previous category (to give boosted candidate Higgs bosons). In each of these categories, a search is made for a broad excess in the reconstructed $\tau\tau$ mass distribution. The main irreducible background, $Z \rightarrow \tau\tau$ production, and the largest reducible backgrounds (W + jets, multijet production, $Z \rightarrow ee$) are evaluated from various control samples in data.

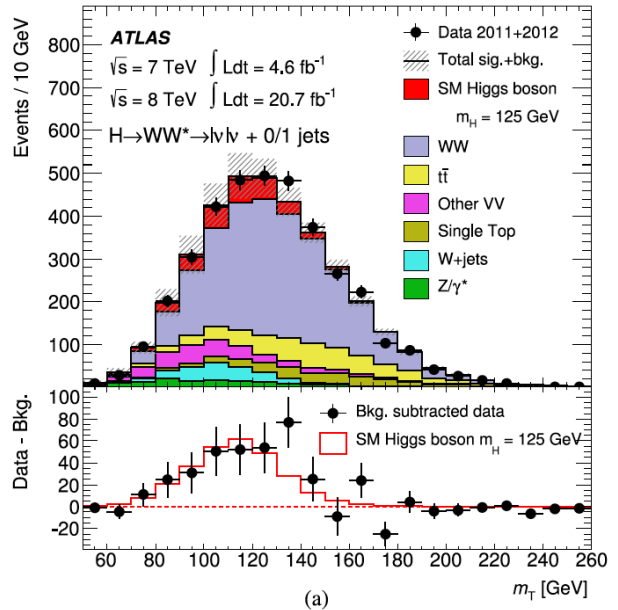
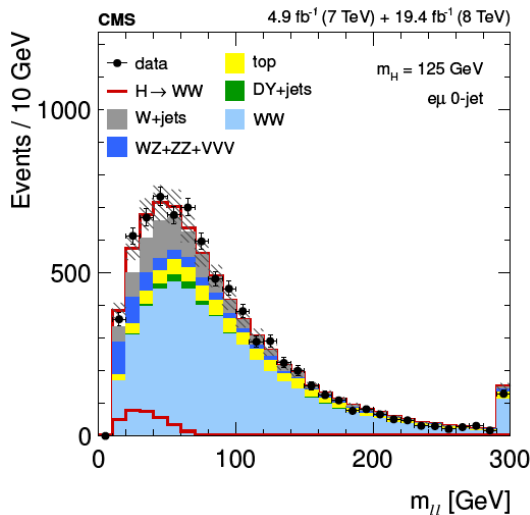


Figure 20: Distribution of dilepton mass in the 0-jet, different-flavor final state in CMS for a $m_H = 125$ GeV SM Higgs boson decaying via $H \rightarrow WW^* \rightarrow l\nu l\nu$ and for the main backgrounds.

Figure 21: The transverse mass distributions for events passing the full selection of the $H \rightarrow WW^* \rightarrow l\nu l\nu$ analysis in ATLAS summed over all lepton flavours for final states with $N_{\text{jet}} \leq 1$. In the lower part the residuals of the data with respect to the estimated background are shown, compared to the expected m_T distribution for a SM Higgs boson.

Figure 22 shows the combined observed and expected di-tau mass distributions from the CMS experiment [33], weighting all distributions in each category of each channel by the ratio between the expected signal and background yields for the respective category in a di-tau mass interval containing 68% of the signal. Figure 23 shows a similar distribution from the ATLAS experiment [34]. In both experiments a small excess of events is seen around $m_H = 125$ GeV. The plots also show the difference between the observed data and expected background distributions, together with the expected distribution for a SM Higgs boson signal with $m_H = 125$ GeV. The observed (expected) significance of the excess with respect to the background only hypothesis at this mass is 3.2 (3.7) standard deviations in the CMS experiment and 4.2 (3.2) standard deviations in the ATLAS experiment. The results include the search for a SM Higgs boson decaying into a τ pair and produced in association with a W or Z boson decaying leptonically.

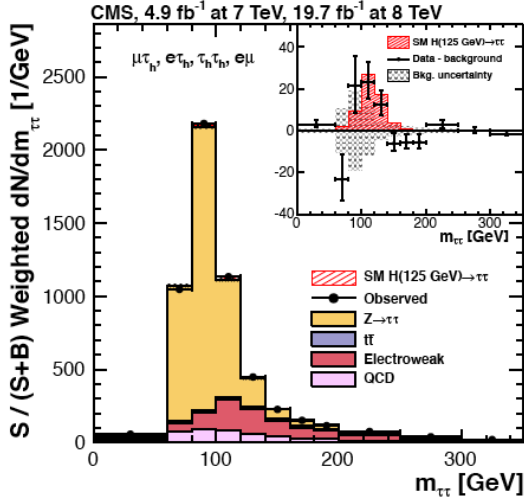


Figure 22: Observed and expected weighted di-tau mass distributions in CMS for the various decay channels combined. The insert shows the difference between the observed data and expected background distributions, together with the expected signal distribution for a SM Higgs boson with $m_H = 125$ GeV.

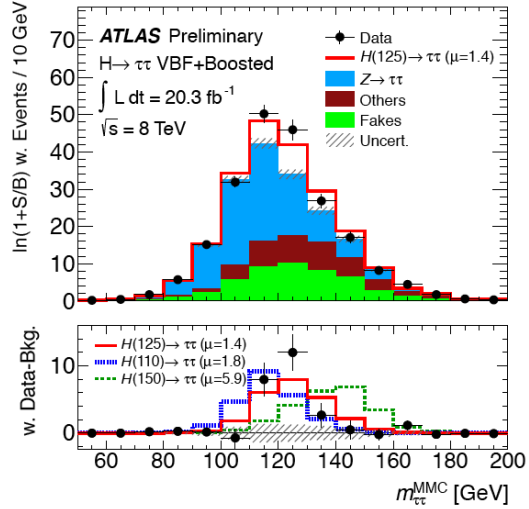


Figure 23: Observed and expected weighted di-tau mass distributions in ATLAS for the various decay channels combined. The bottom panel shows the difference between weighted data events and weighted background events (points) compared to signal events yields for various masses, with signal strengths set to their best-fit values.

6.2.4 $H \rightarrow b\bar{b}$ decay mode

The $H \rightarrow b\bar{b}$ decay mode has by far the largest branching ratio ($\sim 55\%$). However, since $\sigma_{b\bar{b}}(\text{QCD}) \sim 10^7 \times \sigma(H \rightarrow b\bar{b})$, the search concentrates on Higgs boson production in association with a W or Z boson which decay leptonically i.e. $W \rightarrow e\nu/\mu\nu$ and $Z \rightarrow ee/\mu\mu/\nu\nu$.

The $Z \rightarrow \nu\nu$ decay is identified by the requirement of a large missing transverse energy. The Higgs boson candidate is reconstructed by requiring two b-tagged jets. The search is divided into events where the vector bosons have medium or large transverse momentum and recoil away from the candidate Higgs boson.

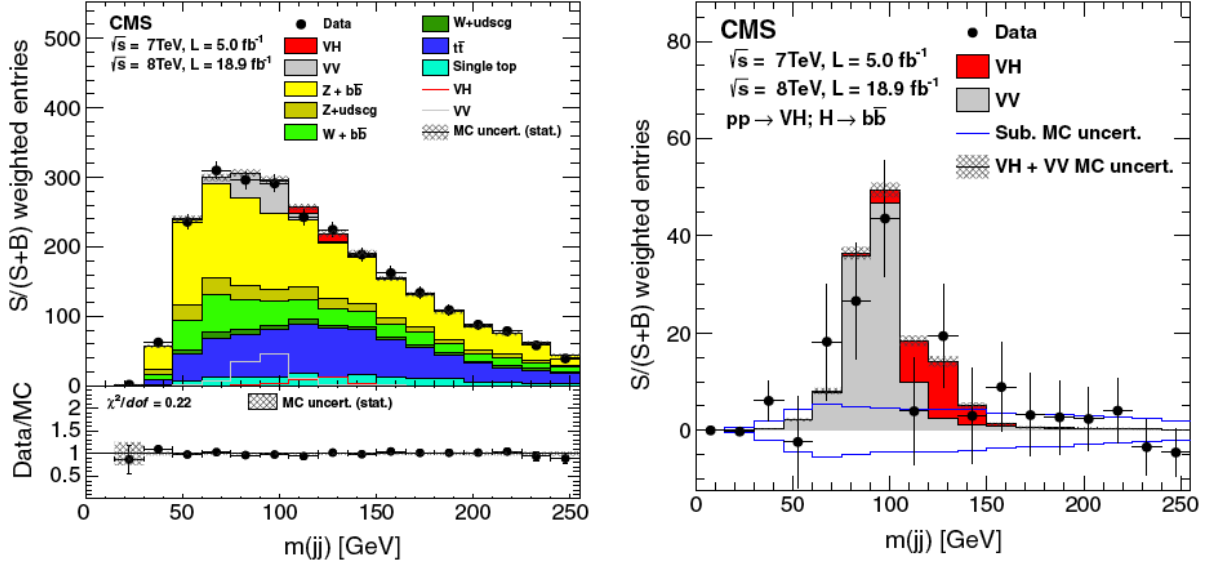


Figure 24: Left: weighted dijet invariant mass distribution in CMS, combined over all channels. The expected signal corresponds to the production of the SM Higgs boson with mass of 125 GeV. The solid histograms for the backgrounds and the signal are summed cumulatively. The panel below shows the ratio of the number of events in data to that of the Monte Carlo prediction for signal and backgrounds. Right: same distribution with all backgrounds, except diboson production, subtracted.

Figure 24 shows the weighted dijet invariant mass distribution in CMS [35] when all backgrounds, except diboson production, are subtracted. The expected signal for a Higgs boson with a mass of 125 GeV is also shown. The data are consistent with the presence of a di-boson signal (ZZ and WZ , with $Z \rightarrow b\bar{b}$), with a small excess consistent with that originating from the production of a 125 GeV SM Higgs boson. For a Higgs boson of mass 125 GeV the excess corresponds to an observed (expected) local significance of 2.1 (2.1) standard deviations.

7. Higgs boson measurements

The detection of significant excesses of events by both experiments around a mass of 125 GeV in several different final states leaves no doubt that a new particle was discovered. Combining all channels discussed in the previous Section, the probability that the observed signal is instead due to upward fluctuations of the backgrounds is about 10^{-24} , corresponding to a total signal significance of more than 10σ per experiment.

Following the announcement of the discovery in July 2012, ATLAS and CMS have been measuring the properties of the new particle with increasing precision and scope. For instance, using the highest-resolution channels, $H \rightarrow \gamma\gamma$ and the $H \rightarrow 4l$, the mass is determined to be: $m_H = 125.36 \pm 0.37$ (stat.) ± 0.18 (syst.) GeV by ATLAS [36] and $m_H =$

125.03 ± 0.27 (stat.) ± 0.14 (syst.) GeV by CMS [37].

Besides the precise measurement of the mass, the two primary questions to ask are: Is the new particle a Higgs boson? If this is the case, is it the Standard Model Higgs boson or a Higgs boson belonging to a more general theory?

Concerning the first question, a particle of the type ‘‘Higgs boson’’ is a very special one, intrinsically different from all others observed so far; it is neither a matter particle nor a force carrier. Two ‘‘fingerprints’’ distinguish it. First, to accomplish its job, a Higgs boson has to interact with the other elementary particles with strengths proportional to their masses, as predicted by the Brout-Englert-Higgs mechanism and as already mentioned in Section 6. The LHC measurements (Fig. 25) indicate that the couplings of the new particle are indeed proportional to mass over a broad range, spanning from the τ -lepton (mass about 1.8 GeV) to the top quark (mass about 100 times larger). Figure 26 further shows that, within the present 15% uncertainties, the measured production rates of the new particle in the various decay channels are in agreement with the predictions for a SM Higgs boson. The combination over all channels of the ratios between measurements and SM expectations gives $\mu=1.00 \pm 0.13$ from CMS [37] and $\mu=1.30 \pm 0.18$ from ATLAS [38].

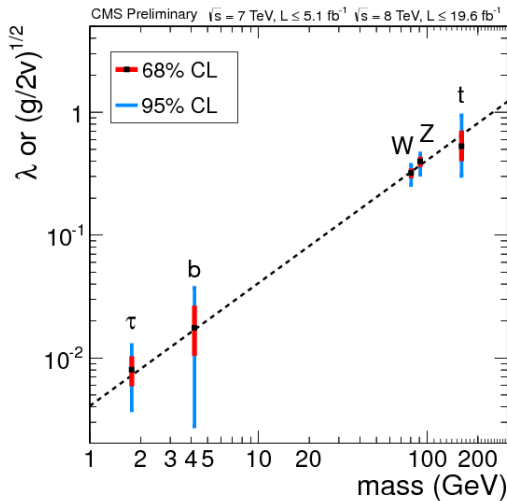


Figure 25: Couplings of the new particle to fermions and bosons as a function of their masses, as measured by CMS. For fermions, the value of the coupling vertex Hff is shown, while for vector bosons the square root of the coupling vertex HVV divided by twice the vacuum expectation value of the Higgs boson field (v) is shown.

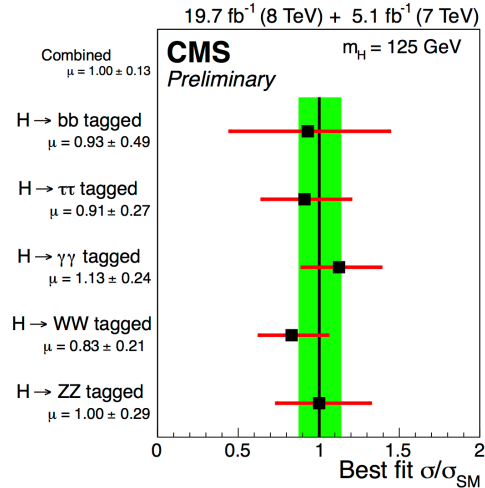


Figure 26: Production rates of the new particle in various decay channels, as measured by CMS, divided by the expectations for a SM Higgs boson [37]. The vertical green band shows the SM prediction with its uncertainty. The combined value is also indicated.

The second fingerprint of a Higgs boson is its spin. Unlike matter particles, which are spin- $1/2$ fermions, and force carriers, which are spin-1 bosons, a Higgs boson is a scalar, i.e. a spin-0 positive-parity ($J^P=0^+$) particle. The spin-parity of a particle can be inferred from the angular distributions of its decay products in the final state, which carry the imprint of the parent particle’s spin. Figure 27 presents the distribution of the polar angle θ^* of the diphoton system with respect to the z -axis of the Collins-Soper frame [39] for events in the signal peak ($122 < m_{\gamma\gamma} < 130$ GeV) of the spectrum shown in Fig. 18. The data are compared to the expectations

for a spin-0 and a spin-2 particle. Although the statistical uncertainties on the experimental points are large, it is nonetheless evident that the data favour the spin-0 over the spin-2 hypothesis. A quantitative likelihood analysis, based on more information and on the combination of the $H \rightarrow \gamma\gamma$, $H \rightarrow 4l$ and $H \rightarrow l\nu l\nu$ final states, shows that the spin-0 hypothesis is strongly preferred by both experiments, with the alternative $J^P = 0^-, 1^+, 1^-, 2^+$ hypotheses rejected with confidence levels larger than 97.8% [40, 41].

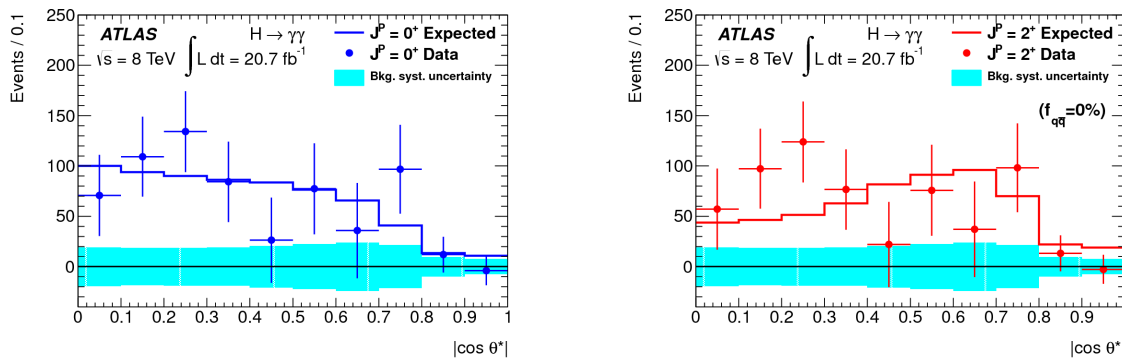


Figure 27: The distributions of the diphoton polar angle (see text) in ATLAS [40] for background-subtracted data in the signal region of the $\gamma\gamma$ spectrum. The expected distributions for positive-parity spin-0 (left) and spin-2 (right) signals produced by gluon fusion, normalised to the fitted number of signal events, are overlaid as solid lines. The bands around the horizontal lines at zero show the systematic uncertainties on the background modeling before the fits.

Hence, within the present experimental uncertainties, the new particle is an elementary object matching both fingerprints expected of a Higgs boson. These results have dramatic consequences also for our understanding of the universe evolution. Indeed, according to cosmology, supported also by several experimental observations, the initial, exponential expansion of the universe, called “inflation”, was triggered by a scalar field [42]. The discovery of an elementary Higgs boson is the first experimental demonstration that scalar fields do exist in nature.

7.1 The remaining questions

Although enormous progress has already been made by ATLAS and CMS to pin down the properties of the newly discovered particle, several outstanding questions remain. They will be addressed by the LHC Run 2, starting in Spring 2015, by the LHC luminosity upgrades [43], and by possible future colliders [44].

Improved measurements of the properties of the new particle, including the observation of rare decays such as $H \rightarrow \mu\mu$, will provide more definitive information about its nature (e.g. whether it is elementary or composite), and offer a doorway to new physics. Indeed, physics beyond the Standard Model is expected to modify the Higgs boson couplings to fermions and bosons by up to a few percent, depending on the energy scale of the new physics; hence experimental precisions from a few permil to a few percent are required to detect significant deviations from the SM expectations.

Higgs boson self-couplings, which would give access to the scalar potential in the SM Lagrangian, may be observed with the full luminosity of the upgraded LHC (3000 fb^{-1} per experiment).

In parallel, searches for new physics may clarify whether or not the (light) Higgs boson mass is stabilized by a new symmetry. Discovery of additional Higgs bosons will indicate the existence of a more complex Higgs sector.

Finally, a definitive exploration of the electroweak symmetry breaking mechanism requires studies of WW , ZZ and WZ production at high masses of the boson pairs (m_{VV}). Such studies will also provide a powerful “closure test” of the SM. As mentioned in Section 1, in the SM without a Higgs boson, the cross section for the scattering of two gauge bosons diverges with energy, becoming unphysical for $m_{VV} \sim \text{TeV}$. It is therefore crucial to verify that the newly discovered particle restores the good behavior of the theory or, else, unravel any additional dynamics contributing to electroweak symmetry breaking [45].

8. Summary

The discovery of a Higgs boson by the ATLAS and CMS experiments at the LHC represents a giant leap for science, as also recognized by *The Economist* in its issue of July 2012. Such a superb accomplishment is the result of the ingenuity, vision and perseverance of the high-energy physics community, and of more than twenty years of talented, dedicated work of those involved in the LHC projects.

After decades of superb theoretical and experimental efforts, and three years of LHC operation, the Standard Model is now complete. However, the Standard Model is not the ultimate theory of particle physics, as many crucial questions remain unanswered. They include the composition of the universe dark matter, the source of the asymmetry between matter and antimatter, the origin of neutrino masses, the motivation for the light mass of the Higgs boson, the extreme feebleness of gravity compared to the other forces.

In the 10-20 years to come, the (upgraded) LHC and possibly new accelerators will help address some of these questions. Perhaps most importantly, the LHC may tell us what are the right questions to ask and how to move ahead.

References

- [1] From condensed matter to the Standard Model of particle physics, L. Alvarez-Gaume, these proceedings.
- [2] F. Englert and R. Brout, *Phys. Rev. Lett.* **13** (1964) 321.
- [3] P.W. Higgs, *Phys. Lett.* **12** (1964) 132.
- [4] P.W. Higgs, *Phys. Rev. Lett.* **13** (1964) 508.
- [5] G.S. Guralnik, C.R. Hagen, T.W.B. Kibble, *Phys. Rev.* **155** (1967) 1554.
- [6] P.W. Higgs, *Phys. Rev.* **145** (1966) 1156.
- [7] Spontaneous symmetry breaking in gauge theories, T.W.B. Kibble, these proceedings.
- [8] L. Evans (ed.), *The Large Hadron Collider, a Marvel of Technology*, EPFL Press, 2009; L. Evans, P. Bryant (ed.) and *LHC Machine*, JINST **03** (2008) S08001.
- [9] ALEPH, CDF, D0, DELPHI, L3, OPAL, SLD Collaborations, the LEP Electroweak

Working Group, the Tevatron Electroweak Working Group, and the SLD Electroweak and Heavy Flavour Groups, Precision electroweak measurements and constraints on the standard model, CERN PH-EP-2010-095, <http://lepewwg.web.cern.ch/LEPEWWG/plots/winter2012/>, arXiv:1012.2367, 2010, <http://cdsweb.cern.ch/record/1313716>.

[10] The pre-LHC Higgs bosons hunt, G. Dissertori, these proceedings.

[11] ALEPH, DELPHI, L3, OPAL Collaborations, and LEP Working Group for Higgs Boson Searches, Phys. Lett. B 565 (2003) 61.

[12] LHC Higgs Cross Section Working Group, S. Dittmaier, C. Mariotti, G. Passarino, R. Tanaka Eds. <http://arxiv.org/abs/1101.0593> (2011), <http://arxiv.org/abs/1201.3084> (2012).

[13] Towards a Higgs boson: first steps in an incredible journey, CERN Courier, May 2013, <http://cerncourier.com/cws/article/cern/53423>

[14] Journey in the Search for the Higgs Boson: The ATLAS and CMS Experiments at the Large Hadron Collider, M Della Negra, P Jenni and T S Virdee 2012 *Science* **338** 1560.

[15] Genesis of the LHC, C. Llewellyn-Smith, these proceedings.

[16] N. Ellis, T. S. Virdee, Ann. Rev. Nucl. Sci. 44 (1994) 609.

[17] The LHC Detector Challenge, Physics World, Vol. 17, No. 9, (2004); Detectors at LHC, Phys. Rep. 403-404 (2004) 401.

[18] Technical Challenges of LHC Experiments, A. Ball, these proceedings.

[19] ATLAS Collaboration, ATLAS: Letter of Intent, CERN-LHCC-92-004 (1992); Technical Proposal, CERN-LHCC-1994-043 (1994); JINST 3 (2008) S08003.

[20] CMS Collaboration, Letter of Intent, CERN-LHCC-92-003 (1992); Technical Proposal, CERN-LHCC-1994-038 (1994); JINST 3 (2008) S08004.

[21] Searches for Supersymmetry, P. Sphicas, these proceedings.

[22] Searches beyond Supersymmetry, D. Charlton, these proceedings.

[23] The technical challenges of the LHC, P. Collier, these proceedings.

[24] The pre-LHC Higgs hunt, G. Dissertori, these proceedings.

[25] ATLAS Collaboration and CMS Collaboration, “Combination of ATLAS and CMS results on the mass of the top quark using up to 4.9 fb^{-1} of $\sqrt{s}=7 \text{ TeV}$ LHC data”, ATLAS-CONF-2013-102, CMS PAS TOP 13-005, September 2013, <http://cds.cern.ch/record/1601811/files/ATLAS-CONF-2013-102.pdf>.

[26] CMS Collaboration, “Measurement of the double-differential inclusive jet cross section at $\sqrt{s}=8 \text{ TeV}$ with the CMS detector”, CMS PAS SMP-12-012, November 2013, <https://cds.cern.ch/record/1547589/files/SMP-12-012-pas.pdf>.

[27] ATLAS Collaboration, Phys. Lett. B 716 (2012) 1.

[28] CMS Collaboration, Phys. Lett. B 716 (2012) 30.

[29] ATLAS Collaboration, Phys. Lett., B 726(2013)88.

[30] CMS Collaboration, CMS-HIG-13-002, arXiv:1312.5353 (2013).

[31] CMS Collaboration, CMS PAS HIG-13-001 (2013).

- [32] CMS Collaboration, JHEP 01(2014)096.
- [33] CMS Collaboration, CMS HIG-13-004, arXiv:1401.5041, 2014.
- [34] ATLAS Collaboration, “Evidence for Higgs Boson Decays to the $\tau\tau$ Final State with the ATLAS Detector”, ATLAS-CONF-2013-108, November 2013, <http://cds.cern.ch/record/1632191/files/ATLAS-CONF-2013-108.pdf>
- [35] CMS Collaboration, Phys. Rev. D 89(2014) 012003.
- [36] ATLAS Collaboration, “Measurement of the Higgs boson mass from the $H \rightarrow \gamma\gamma$ and $H \rightarrow ZZ^* \rightarrow 4l$ with the ATLAS detector using 25 fb^{-1} of pp collision data”, submitted to Physical Review D, June 2014, <http://arxiv.org/pdf/1406.3827.pdf>.
- [37] CMS Collaboration, “Precise determination of the mass of the Higgs boson and studies of the compatibility of its couplings with the standard model”, CMS-PAS-HIG-14-009, July 2014, <http://cds.cern.ch/record/1728249/files/HIG-14-009-pas.pdf>.
- [38] ATLAS Collaboration, “Updated coupling measurements of the Higgs boson with the ATLAS detector using up to 25 fb^{-1} of proton-proton collision data”, ATLAS-CONF-2014-009, March 2014, <http://cds.cern.ch/record/1670012/files/ATLAS-CONF-2014-009.pdf>.
- [39] J.C. Collins and D.E. Soper, Phys. Rev. D 16 (1997) 2219.
- [40] ATLAS Collaboration, Phys. Lett. B 726 (2013), 120.
- [41] CMS Collaboration, Phys. Rev. Lett. 110 (2013), 081803; CMS Collaboration, “Evidence for a particle decaying to W^+W^- in the fully leptonic final state in a standard model Higgs boson search in pp collisions at the LHC”, CMS-PAS-HIG-13-003, March 2013; CMS Collaboration, “Properties of the observed Higgs-like resonance using the diphoton channel”, CMS-PAS-HIG-13-016, July 2013.
- [42] Higgs and cosmology, M. Shaposhnikov, these proceedings.
- [43] The upgraded ATLAS and CMS detectors and their physics capabilities, O. Buchmüller and P. Wells, these proceedings.
- [44] Future accelerators for Higgs studies, T. Wyatt, these proceedings.
- [45] Beyond the Standard Higgs, C. Grojean, these proceedings.